Seam-weld fatigue design for automotive chassis parts: recent numerical computation improvements

Lorenzo ARMANI[a], Matteo Luca FACCHINETTI[a],
Michel DUCHET[b], Bastien WEBER[b]

[a] PSA Peugeot Citroën, INOVEL parc sud, 78140 Vélizy-Villacoublay, France
[b] ArcelorMittal, voie Romaine, 57283 Maizières-les-Metz, France

Abstract Automotive chassis parts are usually made from steel sheet blanks undergoing a forming process (e.g. simple folding, stamping or hydro-forming) and thus assembled by several welded joints (e.g. standard arc-, spot- and laser-weld). Fatigue strength assessment naturally focuses on weld assemblies, which may be the weakest portion of the overall part and are usually affected by the largest mechanical properties scatter. Fatigue numerical computations of weld assemblies use of the finite element method (FEM): in past decades, more and more detailed concepts have been proposed [Hobbacher (2009)], starting from the coarser nominal stress approach, then developing the so-called "*hot-spot*" stress method, the notch-stress approach down to the details of fracture mechanics techniques. The more detailed the modelling, the more sensitive and effective the method is supposed to be. Anyway, the FEM technique is supposed to be consistent with modelling hypothesis usually applied to steel chassis parts. These are usually modelled under plane stress assumption by 2D shell mesh, whose characteristic size is of some mm, the sheet thickness being from 1 mm up to 4 mm. In this framework, since the early 90s PSA Group has been using the "*hot-spot*" stress method in order to assess fatigue design of arc-weld assemblies [Fayard & al. (1996)]. Despite an overall effectiveness, some particular cases still need a deeper stress analysis in order to achieve successfully the fatigue design. In this paper, we analyze the stress-state at the "*hot-spot*" by considering the stress gradient within the steel sheet, i.e. under the weld toe, as an essential parameter driving the seam-weld fatigue strength. Analytical and numerical computations are supported by experimental fatigue tests which allow us to recover former results of [Fermér & al. (1998)].

1 INTRODUCTION

Fatigue design of weld assemblies still remains of prior concern in the automotive industry, despite of several decades of experimental, theoretical and numerical body of work. A basic web search looking for scientific papers dealing with the keywords "*fatigue*", "*weld*" and "*automotive*" states on over 1000 publications per year. From a global point of view, a single steel body-in-white is achieved thanks to at least 1000 spot welds, whereas front and rear axles are seam-welded on an overall length of several meters, i.e. 1000s millimeters (see figure 1). Facing to such relevant quantities, any reliability analysis is supposed to manage failures. From a local point of view, fatigue strength of any welded joint is of course addressed with basic consistency, which let car manufacturers to design them in a proper way. Nevertheless, on one hand failures may be under-predicted, so that expensive process set-up (e.g. stress relieving, shot-peening, …) are engaged a posteriori in order to recover the desired reliability; on the other hand, over-predicted failures mean a non-lean design, which is a natural target for cost- and mass-killer engineers.

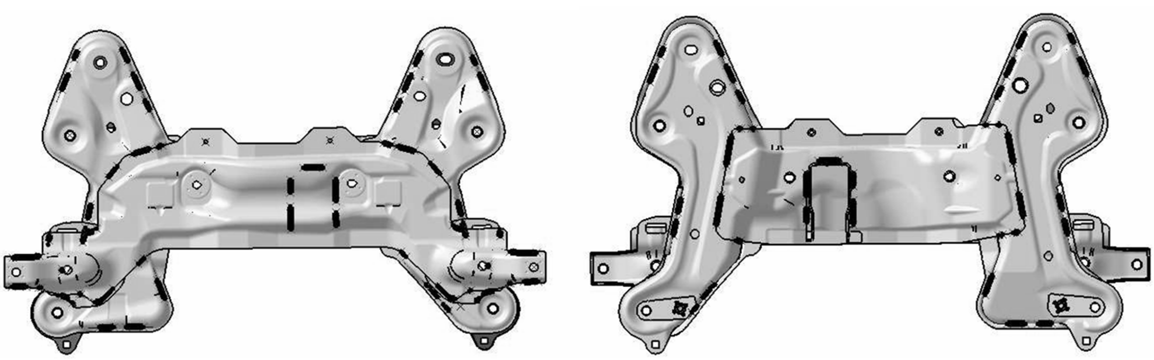

Figure 1. Automotive front axle subframe: seam welds are highlighted in dark grey.
Top view (left side) and bottom view (right side).

In this paper we address the design of standard seam-weld assemblies of steel sheets with respect to high-cycle fatigue. Several fatigue design models may be invoked, as described in comprehensive reviews by [Fricke (2003)], [Radaj & al. (2009)] and [Hobbacher (2009)], the latter in the framework of the International Institute of Welding (IIW). Their application is essentially driven by the characteristic length scale of the concerned structure. For automotive applications, e.g. chassis parts, please note that we usually deal with steel parts of some millimeters thick and up to a meter span (see figure 1), modeled by 2D shell FE of some millimeters mesh size. The coarsest approach considers the whole structure as a bulk and uses of basic structural calculation to calculate nominal stresses: obviously, this is rarely suitable for stamped parts with complex 3D geometry and may be here excluded by default. On the opposite extreme, calling for fracture mechanics concepts and uses of very refined FE models let to compute crack propagation kinematics, which is of prior interest considering that the crack propagation phase is typically longer than the crack initiation phase for welded joints. Actually, this requires the assumption of an a priori crack-like initial imperfection and should need for too expensive FE models to be applied as a standard design method for automotive applications.

Thus, only "*mid-size*" approaches based on stresses directly computed on 2D shell FEM naturally appear affordable when dealing with body-in-white and axle parts. Due to the seam-weld discontinuity, stress fields are expected to be non linear and possibly affected by high or even infinite stress peaks. The usual "*notch-stress*" concept of mechanical engineering may be invoked: its application to seam weld assemblies results in different micro-structural support hypotheses [Radaj & al. (1998), Niemi & al. (2006)], which are usually based on a weld toe radius. Actually, this approach needs for a local stress analysis that is not available with an overall standard mesh size FE model, but calls for specific FE sub-models: an example for automotive application is described in [Sonsino & al. (2012)]. Because of this computational constraint, for pragmatic reasons we privilege and consider here the so-called "*hot-spot stress*" approach.

The idea of excluding the very local stress concentration due to the weld toe using the stress (or strain) at a certain distance away from it lasts to the early 1960s, but effective applications for the automotive industry are published only several decades later by [Fayard & al. (1996)] for PSA Peugeot Citroën company, [Fermér & al. (1998)] for VOLVO Cars Corporation, [Savaidis & al. (2000)] for MAN Group and more recently [Turlier & al. (2010)] for LOHR industries. The "*hot-spot stress*", also known as structural or geometric stress, is nothing but a fictitious stress value calculated in the vicinity of the weld toe and following an extrapolation rule from other stress values slightly away from it. This is sufficient to appreciate the stress increase due to the particular structural configuration of the weld assembly, i.e. a sort of "*global notch effect*", and avoids the shortcomings of the "*local notch effect*" approach presented above. Obviously, the method effectiveness is submitted to the consistency between experimental measures (i.e. strain gage location) and related FEM mesh rules (i.e. integration point location): this result in several proposals, as described by the above references and the general design recommendations provided by the International Institute of Welding (IIW) [23], the Eurocodes (EC3) [20], the British Standard (BS) [19] and the Forschungs Kuratorium Maschinenbau (FKM) guidelines [21], respectively. Please note that, according to [Dong (2001)], the ratio between the "*hot-spot stress*" to the nominal one leads to the identification of two types of weld assemblies, associated to more or less steep stress gradients approaching to the weld toe.

The fatigue resistance is not discussed here considering the welding process quality and scatter: nominal, supervised welding parameters and conditions are assumed a priori, which is supposed consistent with highly automated welding workshops. Moreover, no process effect is explicitly taken into account: even if there is evidence at least of base material mechanical properties changes and of residual stress in the vicinity of any seam-weld, and process numerical simulation is from now on affordable and reliable [Bristiel (2009), Garsot & al. (2011)]. The fatigue resistance is not argued any more with respect to the load time-history, i.e. the influence of the stress ratio (or mean load effect) and the proportionality (or not) of the loading path. In the sequel, we will address seam weld fatigue failures occurring at the weld toe only, thus neglecting a priori any root cracking: this choice is relevant if the design practice avoid locating the maximum stress concentration at the weld root, thus letting non destructive crack detection by standard inspection on the visible side of the fillet weld (see figure 2).

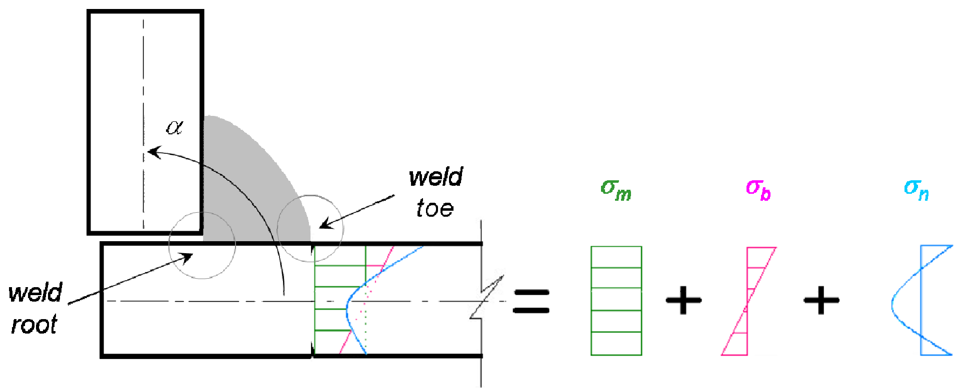

Figure 2. T-fillet weld. Assembly section (left side) and weld toe stress decomposition (right side).

Within such a complex framework, the present paper is organized as follows. Chapter 2 relates how the stress analysis at the weld toe is expected to be improved, relating to both fatigue test specimens and chassis parts. Thus, chapter 3 particularly addresses the effects of the stress gradient within the sheet thickness at the weld toe, from the computational and the experimental points of view, respectively. Conclusions and perspectives end, chapter 4.

2 WELD TOE STRESS ANALYSIS

Let us consider a fillet seam weld undergoing high-cycle fatigue. Figure 2 shows the most representative seam weld assembly applied to automotive front and rear axles, the angle α possibly varying from 90° (T-fillet weld) up to 180° (plate lap fillet weld or overlap). As explained before, the stress state at the weld toe is expected to be the significant fatigue stress of the overall weld assembly.

Each "*hot-spot stress*" approach implies specific rules to be applied [Doerk (2003), Niemi (2006)], dealing with:

- FE mesh constraints: e.g. element size, type and formulation;
- physical variables to be analyzed: e.g. the so-called "*VOLVO method*" [Fermér & al. (1998)] uses of nodal forces, the "*PSA method*" [Fayard & al. (1996)] works on surface centroid integration point stresses, whereas [Dong (2001)] is based on the overall through-thickness stress distribution;
- extrapolation to be applied in order to evaluate a reliable "*hot-spot stress*": e.g. linear, non-linear. Please note that [Dong (2001)] identifies two types of weld assemblies depending on the stress gradient approaching to the weld toe, considering the ratio between the "*hot-spot stress*" to the nominal one.

No matter of all these rules, in the sequel we discuss the stress state in the vicinity of the weld toe in order to improve the fatigue design of any "*hot-spot stress*" method. Even neglecting any effect of the load time-history, i.e. the influence of the stress ratio and the proportionality of the loading path, many aspects are supposed to be addressed. We assume here a priori a plane stress state, basically because of dealing with thin steel sheets modeled by 2D shell FE and. Actually, even considering local 3D effects at the weld toe, the steel sheet surface concerned by the "*hot-spot stress*" method is a free surface. Particular attention is devoted to the stress analysis comparison between a wide range of weld assemblies on axle parts (see figure 1) and welded specimens used in elementary fatigue tests. The basic one considered here has a plate lap fillet seam (see figure 3): at first, it is welded on almost the overall width of the sheet, then it is machined on both sides in order to drive any fatigue failure to the seam and avoid any edge effect. Please note that the specimen is completed with two wedges to let it be properly tightened in the testing machine jaws. The usual specimen slenderness is of about $L / e \sim 100$.

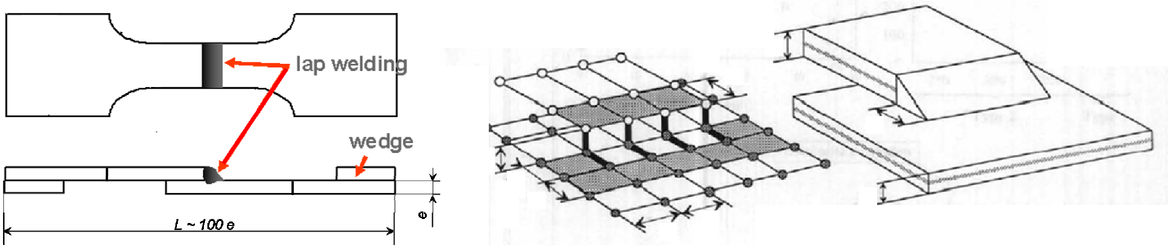

Figure 3. Basic fatigue test specimen: geometry (left side) and FE model (right side).

2.1 Multi-axial stress state

In continuum mechanics and in the framework of Cauchy stresses [24], a general purpose tri-axial stress rate, T_r is defined by the dimensionless ratio of the first stress invariant (i.e. the hydrostatic pressure, p_h) on the second stress invariant (e.g. the Von Mises equivalent stress, σ_{VM}):

$$T_r = \frac{p_h}{\sigma_{VM}} \quad (1)$$

Thus, the sign of the tri-axial stress rate depends on the on the tensile/compression load mode and its value is bounded between ±2/3 under the hypothesis of plane stress state. In particular, a pure shear stress leads to $T_r = 0$, uni-axial stress corresponds to $T_r = \pm 1/3$ and equi-bi-axial stress implies $T_r = \pm 2/3$. The extensive application of such an analysis in the vicinity of the weld toe, at any time during a cyclic fatigue load, leads to the following considerations (see figure 4 – left side):

- axle parts weld assemblies are observed to experience almost any possible multi-axial stress rate, except for strong bi-axial and pure shear stresses;
- a basic fatigue test specimen like the one in figure 3 is supposed to undergo almost uni-axial stress, a minor bi-axial behaviour being associated to non-linear anticlastic bending and free edge effects;
- the four fatigue test specimens considered by [Fayard & al. (1996)] span a wider range of multi-axial stress state, but without covering all experienced axle part stress states.

Thus, even if perfect consistency is guaranteed between experimental versus computational stress measurement, in the framework of any "*hot-spot stress*" method, the choice of the fatigue test specimens is crucial in order to recover the stress state experienced by axle parts. Please note that any attention on the weld assembly multi-axial stress rate is submitted to the capability of the fatigue design criterion to afford it.

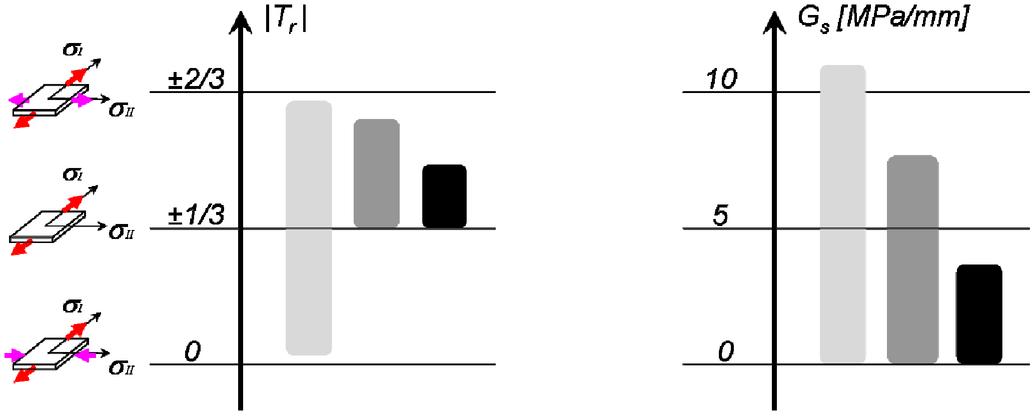

Figure 4. Tri-axial stress rate at the weld toe, T_r (left side), and stress gradient along the seam weld, G_s (right side) for: axle parts weld assemblies (light grey), fatigue test specimens considered by [Fayard & al. (1996)] (dark grey), basic fatigue test specimen (black).

2.2 Stress gradient along the seam weld

Let us consider the variation of the stress state along the seam weld. Be s the curvilinear coordinate following the seam weld and σ any significant scalar stress measured at the weld toe, e.g. the stress tensor component normal to the local s direction. Thus, a stress gradient is defined as:

$$G_s = \frac{\partial \sigma}{\partial s} \qquad (2)$$

The extensive application of such an analysis in the vicinity of the weld toe, at any time during a cyclic fatigue load, leads to the following considerations (see figure 4 – right side):

- axle parts weld assemblies are observed to experience stress gradients over 10 MPa/mm;
- a basic fatigue test specimen like the one in figure 3 undergoes virtually zero stress gradient. In fact, due to non-linear anticlastic bending and free edge effects, a stress gradient up to some MPa/mm is observed;
- the four fatigue test specimens considered by [Fayard & al. (1996)] are expected to span stress gradients over 5 MPa /mm.

Again, even if common design rules try to minimize local stress gradients, the choice of the fatigue test specimens is crucial in order to recover the stress state experienced by axle parts. Please note that a stress gradient of about 10 MPa/mm corresponds to 50 MPa within adjacent elements whose mesh size is of about 5 mm. These orders of magnitude are supposed to be compared to standard stress gradients in any FEM analysis.

2.3 Stress gradient within the sheet thickness

The stress state at the weld toe may be considered as a superposition of elementary loads (see figure 2), i.e. membrane stress, σ_m and bending stress, σ_b . Please remember that this framework is supposed to account for "*global notch effect*", i.e. the stress increase due to the structural configuration of the weld assembly, but neglects any "*local notch effect*", σ_n , i.e. the non-linear stress increase due to the detailed weld geometry, which may be appreciated only by a "*notch-stress method*". Following this analysis, any weld assembly may be considered as a:

- "*stiff*" joint: if the stress state is dominated by membrane-mode load, i.e. the stress distribution through the sheet thickness at the weld toe is almost uniform;
- "*flex*" joint: if the stress state is dominated by bending-mode load, i.e. the stress distribution through the sheet thickness at the weld toe is butterfly-like.

Please note that this behaviour is an issue of both the weld assembly geometry (e.g. sheet thickness versus assembly slenderness) and the applied load (e.g. forces versus momentum). For the sake of classification, [Fermér & al. (1998)] define a dimensionless stress gradient within the sheet thickness, r :

$$r = \frac{|\sigma_b|}{|\sigma_b| + |\sigma_m|} \quad (3)$$

Referring to figure 5, it is bounded and effective in order to identify the dominant load at the weld toe. The extensive application of such an analysis in the vicinity of the weld toe, at any time during a cyclic fatigue load, leads to the following considerations (see figure 5):

- axle parts weld assemblies are observed to experience almost all the possible r values. Again, please note that the "*flex*" / "*stiff*" behaviour is an issue of both the weld assembly geometry (e.g. sheet thickness versus assembly slenderness) and the applied load (e.g. forces versus momentum) ;
- a basic fatigue test specimen like the one in figure 3 is more likely dominated by bending-mode load. Actually, even if the macroscopic load is a pure membrane load, aligned along the specimen axes thanks to a couple of wedges, basic continuum mechanics prove that the stress distribution is not supposed to be uniform any more. At last, this may be magnified by the geometry slenderness ;
- the four fatigue test specimens considered by [Fayard & al. (1996)] are expected to span a wider range of stress gradients than any basic fatigue specimen, but without covering all possible r values.

As stated in the previous paragraphs, the choice of the fatigue test specimens is crucial in order to recover the stress state experienced by axle parts.

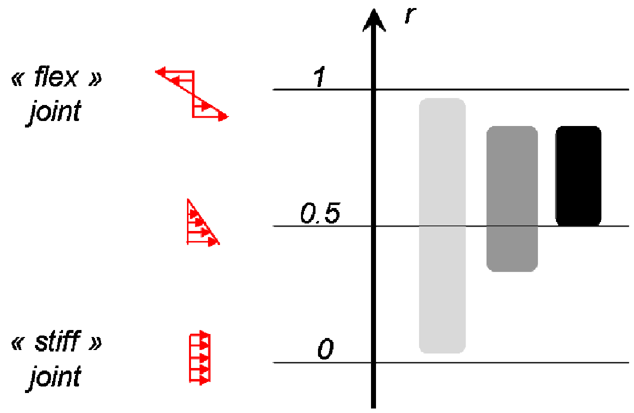

Figure 5. Stress gradient within the sheet thickness, r for: axle parts weld assemblies (light grey), fatigue test specimens considered by [Fayard & al. (1996)] (dark grey), basic fatigue test specimen (black).

3 FATIGUE EFFECTS OF "*r*" STRESS GRADIENT

The three scalar parameters discussed above, the tri-axial stress rate, T_r (§2.1), the stress gradient along the weld seam, G_s (§2.2) and the stress gradient within the sheet thickness, r (§2.3), are expected to improve the weld toe stress analysis in any fatigue design framework. All these three scalars provide a photograph of the stress field in the vicinity of the weld toe, at any time during a cyclic fatigue load. Actually, the first two consider the mechanical behaviour of the seam weld along the welded surface, whereas the last one concerns with a section orthogonal to the seam weld line. Because of dealing with homogeneous stress state along the weld is easier to manage, particularly from the experimental point of view, at present we only focus on fatigue effects of the stress gradient within the sheet thickness.

3.1 Literature data

Since the seminal work of [Fermér & al. (1998)], the dimensionless stress gradient within the sheet thickness, r is associated to different sets of S-N data, i.e. Wöhler curves. Actually, for the same number of cycles to failure, N a "*flex*" joint is supposed to experience larger stresses, S than a "*stiff*" one (see figure 6). Let us consider experimental data collected on structures with sheet thickness from 1.0 up to 3.0 mm undergoing fatigue cycles with load ratio R = -1 : for a target number of cycles to failure, N = 10^6 the fatigue strength of a "*flex*" joint is found up to twice the fatigue strength of a "*stiff*" one.

No basic load effect on fatigue strength is supposed to be invoked, because of fatigue failure is expected to occur at the very weld toe, not in the sheet bulk. Nevertheless, this experimental evidence could be inferred from fracture mechanics considerations, as proposed by [Dong (2001)].

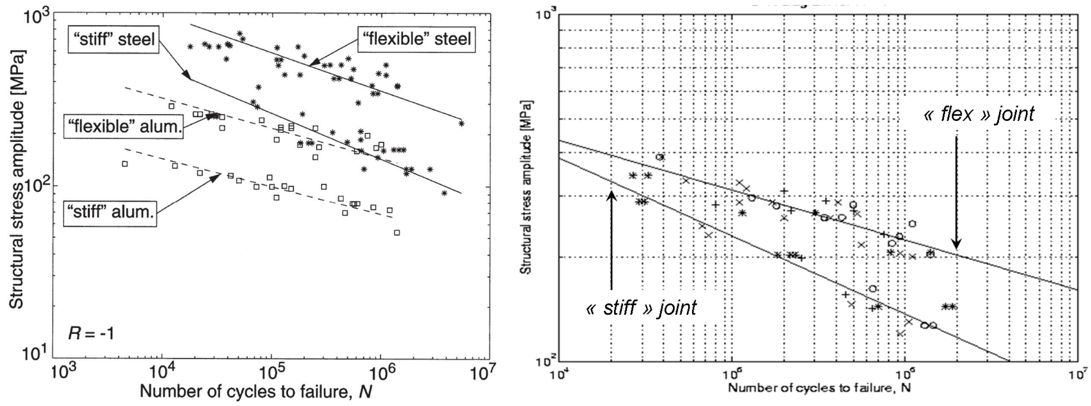

Figure 6. Wöhler curves depending on the stress gradient within the sheet thickness from: [Fermér & al. (2001)] (left side), HBM nCODE user manual [22] (right side). Fatigue loads are collected for structures with sheet thickness from 1.0 up to 3.0 mm undergoing fatigue cycles with load ratio R = -1.

3.2 Specimen stress state analysis

Let us now consider a basic welded fatigue test specimen (see figure 3). Even if the specimen:

- is completed with two wedges to let it be properly tightened in the testing machine jaws,
- is perfectly centered and aligned with respect to the fatigue machine axis,
- is submitted to a pure traction load,
- undergoes an almost spanwise uniform stress state along the lap filled seam weld,

fatigue strength scatter data are expected to be significantly affected as r may spans from 0 up to 1, depending on specimen slenderness and boundary conditions. In the sequel, we address this crucial point by different approaches: analytical calculations (§3.2.1), FE computations (§3.2.2) and experimental tests (§3.2.3).

The specimen is welded from a high strength steel sheet 2.0 mm thick and has an overall length of about $L \sim 100\ e$. The material is assumed to be homogeneous and isotropic, with linear elastic behaviour modelled by standard Young modulus, $E = 210$ GPa and Poisson coefficient, $\nu = 0.3$. Please note that positive load ratios (e.g. $R = 0.1$) are preferred for such a specimen, in order to avoid any buckling problem under compression load: thus, a standard Haigh correction may be used to compare with basic alternate load fatigue data (i.e. $R = -1$).

3.2.1 Analytical approach

The stress state at the weld toe is calculated applying basic continuum mechanics, under the following hypotheses: plane stress state, small linear strain and negligible displacement around the initial undeformed position. Inferring the static equilibrium, the (linear and monotonic) stress distribution within the sheet thickness is a closed form solution depending on the applied axial force, F and the moment, M so that:

$$F = \int_{-e/2}^{+e/2} \sigma(z)\,dz \quad , \quad M = \int_{-e/2}^{+e/2} \sigma(z)\,z\,dz \qquad (4)$$

z being the coordinate through the sheet. In this framework, r depends only on M, the specimen slenderness influence being worthless. Actually, please note that no solution virtually exists with vanishing moment, M = 0. Thus, even if the fatigue machine is supposed to apply a pure traction load, a moment is expected to be countered anyway.

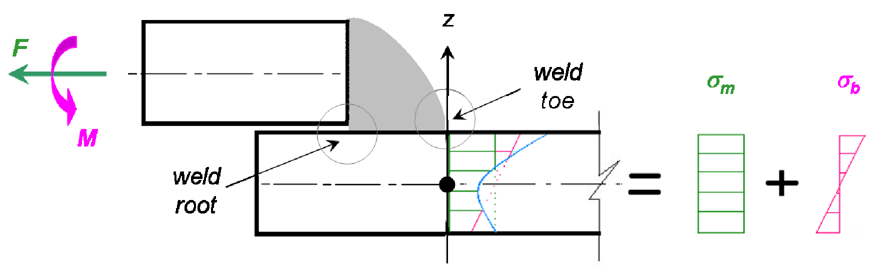

Figure 7. Plate lap fillet weld or overlap. Applied load (left side) and weld toe stress decomposition (right side).

3.2.2 FE approach

The stress state at the weld toe is computed by FEA using the commercial solver ABAQUS [18]. At first, a 2D mesh according to "*PSA method*" is considered (see figure 2), using linear shell elements involving reduced integration and three integration points within the sheet thickness; then a more refined 3D mesh using linear solid elements is used in order to confirm previous coarser results (see figure 8). In this framework, non-linear large displacements may effectively be taken into account and the use of the option NLGEOM does influence the computed results indeed, depending on the specimen slenderness. Moreover, different boundary conditions are assessed: perfect clamping in the testing machine jaws is compared to the use of pivoting hinges.

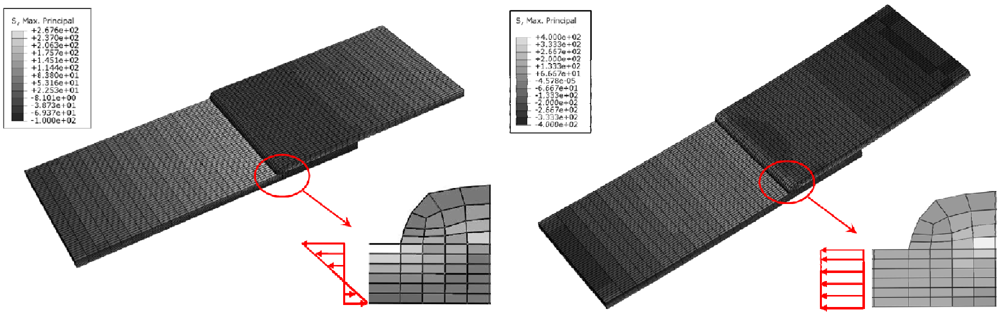

Figure 8. Non-linear 3D FEA. Evidence of maximum stress at the weld toe for both "flex" joint (left side) and "stiff" joint (right side). Stress intensity increases from dark grey to light grey.

First of all, evidence of the weld toe experiencing the maximum stress is confirmed for both "*flex*" and "*stiff*" joints, as shown in the figures above. Moreover, as already highlighted by the analytical approach, even if the first integral of equation (4) is invariant since controlled by the fatigue machine, the stress state within the sheet thickness at the weld toe may deeply vary as a consequence of the induced moment. Thus, for the same nominal stress, the significant stress at the weld toe may be magnified leading to different fatigue strength.

3.2.3 Experimental approach

Previous FEA needs to be assessed by experimental results. A comprehensive fatigue test campaign, for which plate lap filled weld specimens are equipped with specific strain gages (see figure 9), is currently in progress in order to check, respectively:

- the influence of the specimen slenderness and clamping conditions on the weld stress state,
- the "*PSA method*" reliability in modelling the stress state at the weld toe.

Figure 9. Fatigue test specimens: plate lap fillet weld equipped with specific strain gages.

4 CONCLUSIONS AND PERSPECTIVES

Fatigue strength of weld assemblies is addressed in this paper, with particular attention to automotive applications. Strong computation constraints drive the use of the so-called "*hot-spot stress*" design method, which account for seam weld fatigue failures occurring at the weld toe only. Within this framework, stress analysis at the weld toe is improved considering three parameters: the tri-axial stress rate, T_r (§2.1), the stress gradient along the weld seam, G_s (§2.2) and the stress gradient within the sheet thickness, r (§2.3).

At first, a comparison between the stress states experienced by axle parts versus fatigue test specimens proves how the choice of the latter is crucial to assess a reliable fatigue design. Then, the weld assembly "*flex*" or "*stiff*" behaviour is recognized as an opportunity for cost- and mass-killer engineers to improve axle parts design, according to previous literature results. Analytical calculations (§3.2.1), FE computations (§3.2.2) and experimental tests (§3.2.3) show that basic specimen fatigue strength strongly depends on its slenderness and boundary conditions.

Unfortunately, fatigue tests are currently in progress as the deadline paper submission is coming. Thus, we apologize for not being able to present here a comprehensive and conclusive analysis. Experimental results are supposed to be discussed versus FE computations at the oral presentation only.

5 REFERENCES

5.1 Books

1. P. Bristiel, Simulation numérique du soudage - Application au cas industriel d'une traverse arrière automobile, éditions des Techniques des Ingénieurs, BM-7-762, 2010
2. K. Dang Van, Macro–micro approach in high-cycle multi-axial fatigue, McDowell DL, Ellis R, editors. Advances in multi-axial fatigue, ASTM STP 1191, Philadelphia, 1993
3. E. Niemi, W. Fricke, S.J. Maddox, Fatigue analysis of welded components: designer's guide to the structural hot-spot stress approach, Woodhead Publishing, 2006
4. D. Radaj, C.M. Sonsino, W. Fricke, Fatigue weld assessment of welded joints by local approaches, Woodhead Publishing, Cambridge, 2006

5.2 Conference Proceedings

5. M. Fermér, M. Andreasson, B. Frodin, Fatigue life prediction of MAG-welded thin-sheet structures, International Body Engineering Conference, Warren, 1998, SAE technical paper, vol. 2, n. 982311
6. N. Garsot, N.T. Niane, P.Bristiel, Simulation numérique du soudage appliquée au cas d'une traverse arrière d'automobile, 20ème Congrès Français de Mécanique, Besançon, 2011
7. D. Turlier, P. Klein, F. Bérard, "Seam Sim" method for seam weld structural assessment within a global structure FEA, 63rd Annual Assembly & International Conference of the International Institute of Welding, Istanbul, 2010

5.3 Journal Articles

8. O. Doerk, W. Fricke, C. Weissenborn, Comparison of different calculation methods for structural stresses at welded joints, International Journal of Fatigue (2003), vol. 25, pp. 359-369
9. P. Dong, A structural stress definition and numerical implementation for fatigue analysis of welded joints, International Journal of Fatigue (2001), vol. 23, pp. 865-876
10. J.L. Fayard, A. Bignonnet, K. Dang Van, Fatigue design criterion for welded structures, Fatigue & Fracture of Engineering Materials & Structures (1996), vol. 15, pp. 723-729
11. W. Fricke, Fatigue analysis of welded joints: state of development, Marine Structures (2003), vol. 16, pp. 185-200
12. A.F. Hobbacher, The new IIW recommendations for fatigue assessment of welded joints and components - A comprehensive code recently updated, International Journal of Fatigue (2009), vol. 31, pp. 50-58
13. I.V. Papadopoulos, Fatigue limit of metals under multi-axial stress conditions: the microscopic approach, Commission of the European Communities, Joint Research Centre, ISEI/IE 2495/93 (1993), technical note No. I.93.101
14. D. Radaj, C.M. Sonsino, W. Fricke, Recent developments in local concepts of fatigue assessment of welded joints, International Journal of Fatigue (2009), vol. 31, pp. 2-11
15. G. Savaidis, M. Vormwald, Hot-spot stress evaluation of fatigue in welded structural connections supported by finite element analysis, International Journal of Fatigue (2000), vol. 22, pp. 85-91
16. C.M. Sonsino, W. Fricke, F. de Bruynec, A. Hoppec, A. Ahmadid, G. Zhang, Fatigue assessment of welded joints: notch-stress concepts – background and applications, International Journal of Fatigue (2012), vol. 34, pp. 2-16

5.4 Dissertations or Thesis

17. J.L. Fayard, Dimensionnement à la fatigue polycyclique de structures soudées, PhD thesis, Ecole Polytechnique, 1996

5.5 Others

18. Abaqus / Standard, v6.7, www.abaqus.com
19. British Standard, BS 7608, Code of practice for fatigue design and assessment of steel structures (1993), www.bsigroup.com
20. Eurocodes, EN 1993-1-9, Design of steel structures - Fatigue strength of steel structures (2005), www.eurocode1.com
21. ForschungsKuratorium Maschinenbau (FKM) guideline, Analytical strength assessment of components in mechanical engineering
22. HBM nCODE, www.ncode.com/en
23. International Institute of Welding (IIW), www.iiw-iis.org
24. Stresses in continuum mechanics, http://en.wikipedia.org/wiki/Stress_(mechanics)